Electronic Supplementary Information (ESI)

Solid state NMR and DFT studies of azo-hydrazone tautomerism in azo dyes and Chitosan-dye films

Coral Hillel,[a] Sarah Collins,[b] Amanpreet Parihar,[b] Ozzy Mermut,[a] Christopher J. Barrett,[a,b] William J. Pietro,[c] and Linda Reven[b]*

Table of Contents

1. Solution NMR spectra for ALR and proton shift assignments

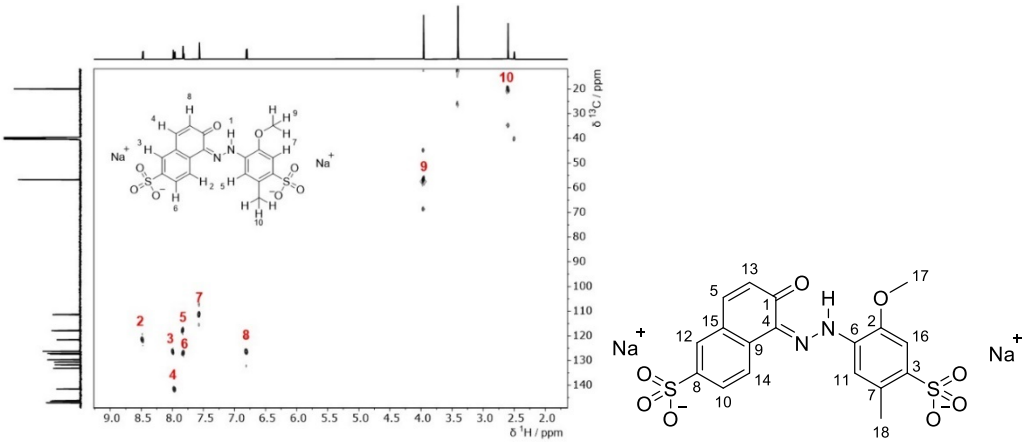

Figure S1 800 MHz ^{1}H-^{13}C HSQC spectrum of ALR in DMSO

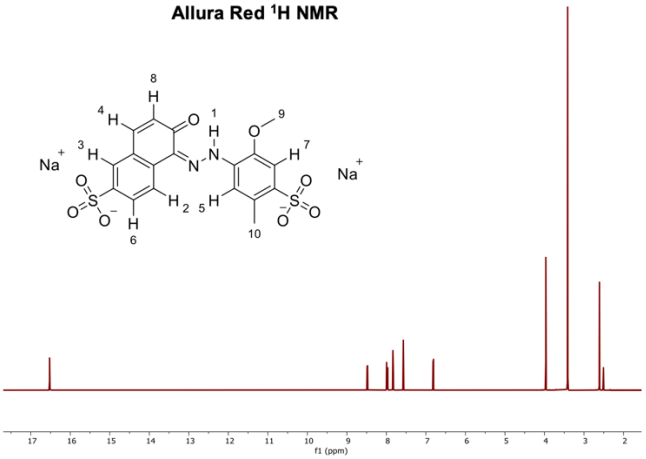

Assignment	Shift (ppm)
1	16.52
2	8.48
3	8.00
4	7.97
5	7.83
6	7.82
7	7.57
8	6.81
9	3.97
10	2.61

Figure S2 800 MHz ^{1}H spectrum of ALR in DMSO

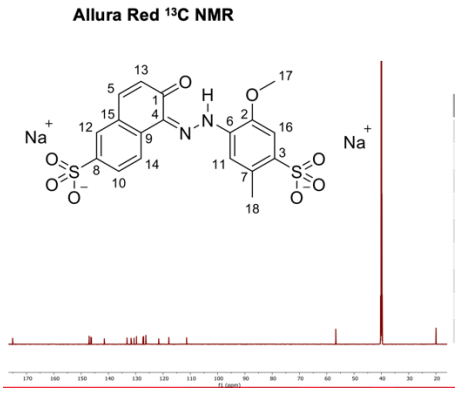

Assignment	Shift (ppm)	Assignment	Shift (ppm)
1	175.11	10	127.34
2	147.09	11	127.12
3	146.45	12	126.33
4	146.25	13	126.28
5	141.51	14	121.57
6	133.17	15	117.89
7	131.71	16	111.36
8	130.60	17	56.70
9	129.73	18	19.95

Figure S3. 400 MHz ^{13}C spectrum of ALR in DMSO

2. Variable temperature $^{1}H–^{15}N$ HMBC spectra

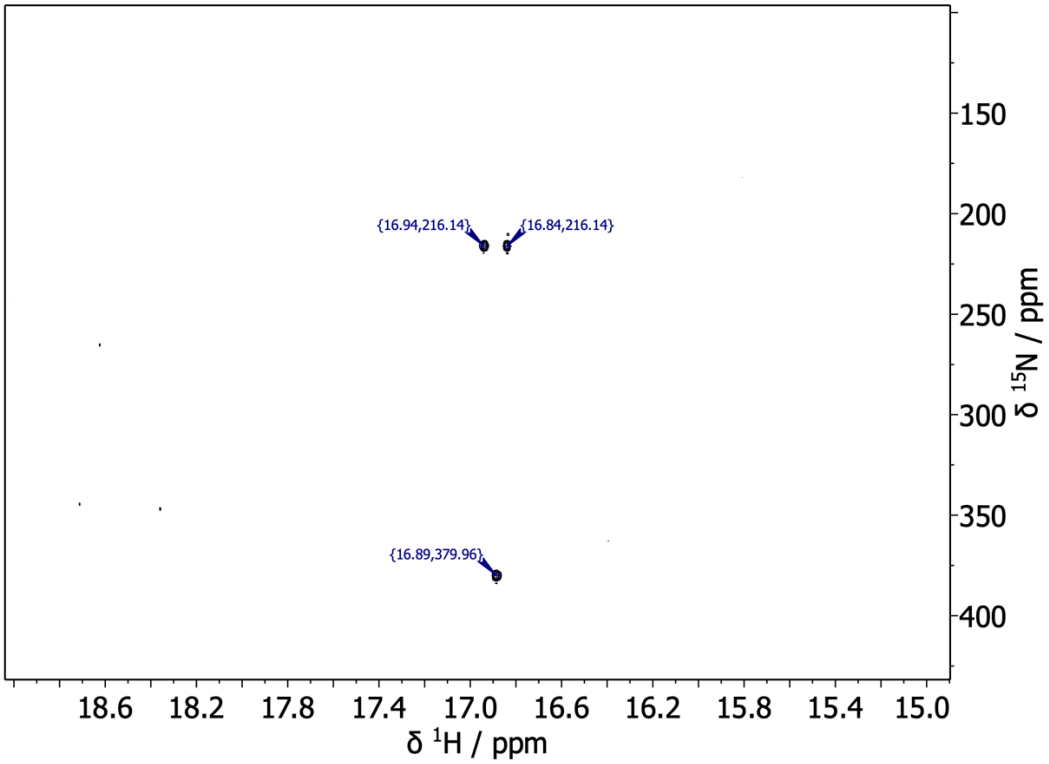

Figure S4. $^{1}H–^{15}N$ HMBC spectrum of ALR at -30.0 °C, measured in DMF.

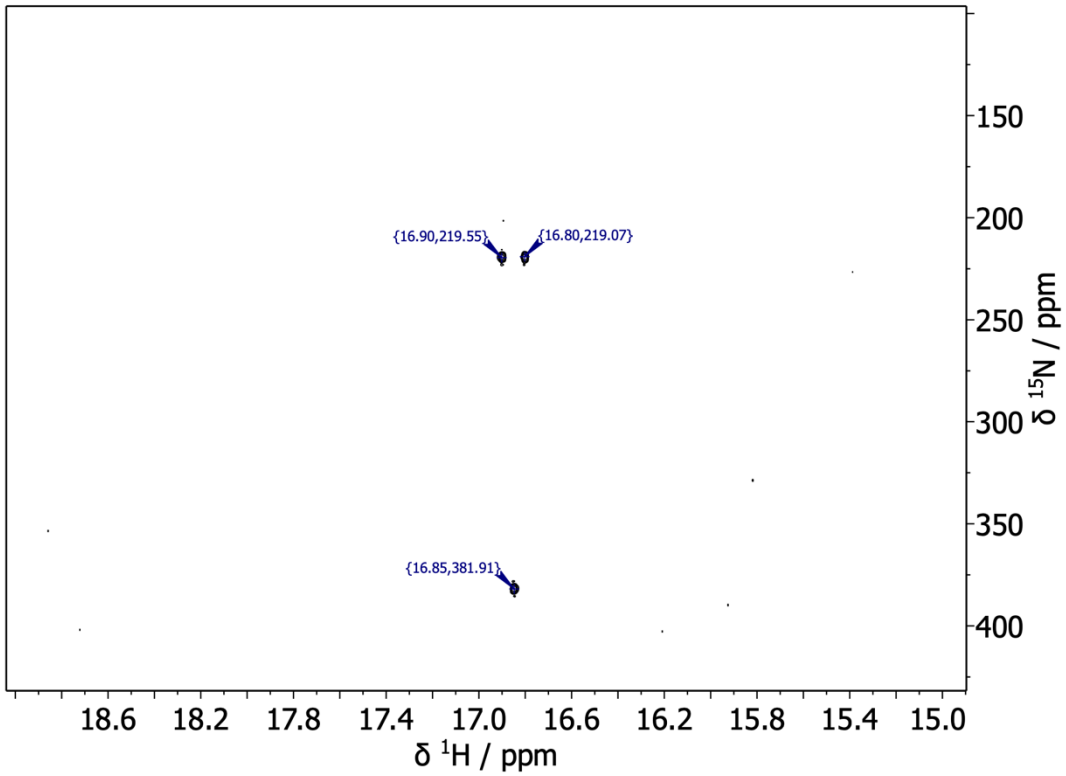

Figure S5. $^{1}H–^{15}N$ HMBC spectrum of ALR at -15.0 °C, measured in DMF.

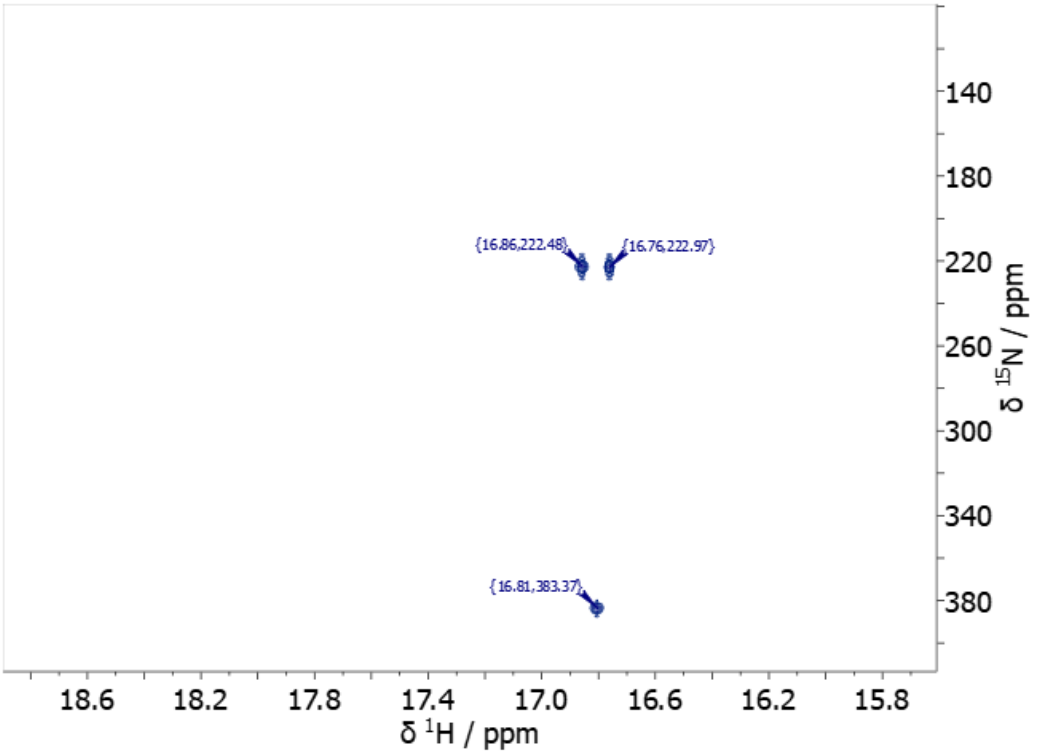

Figure S6. $^{1}H–^{15}N$ HMBC spectrum of ALR at 0 °C, measured in DMF.

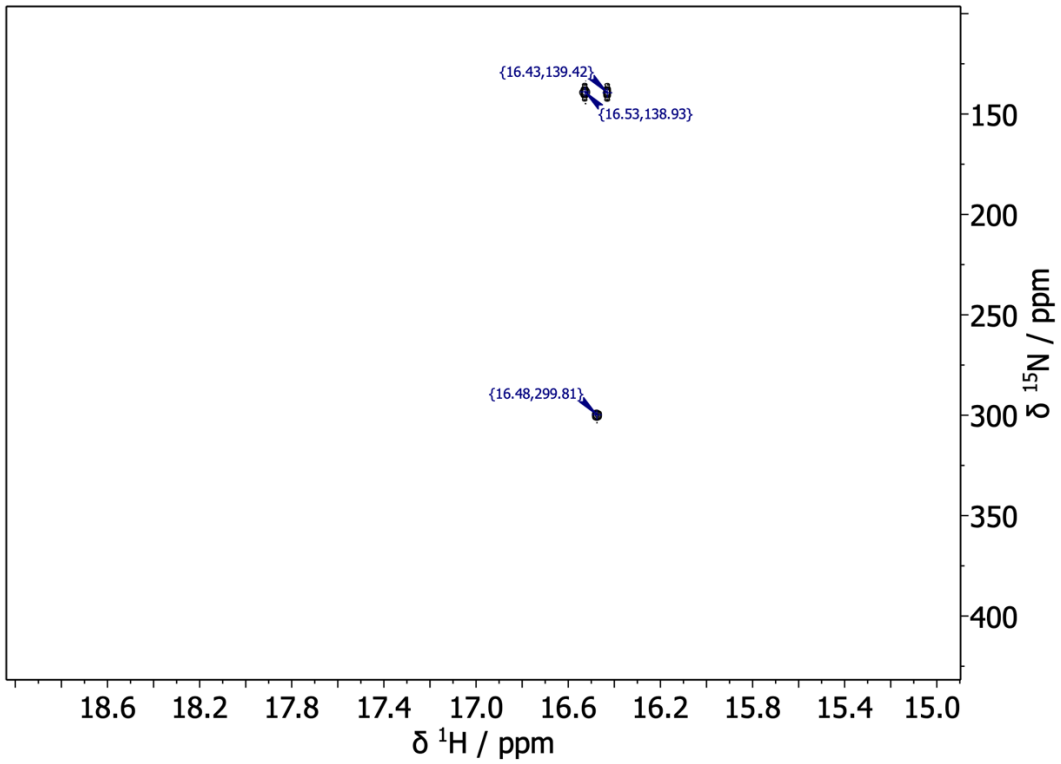

Figure S7. $^{1}H–^{15}N$ HMBC spectrum of ALR at 15 °C, measured in DMF.

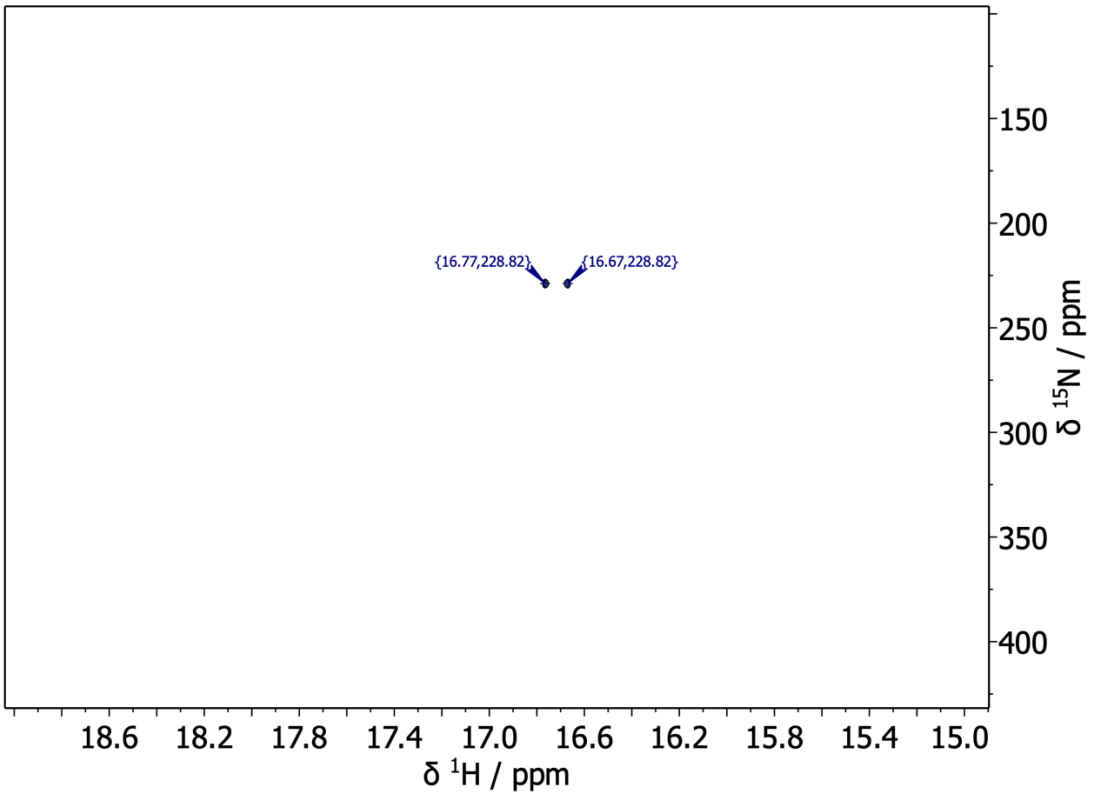

Figure S8. $^{1}H–^{15}N$ HMBC spectrum of ALR at 30 °C, measured in DMF.

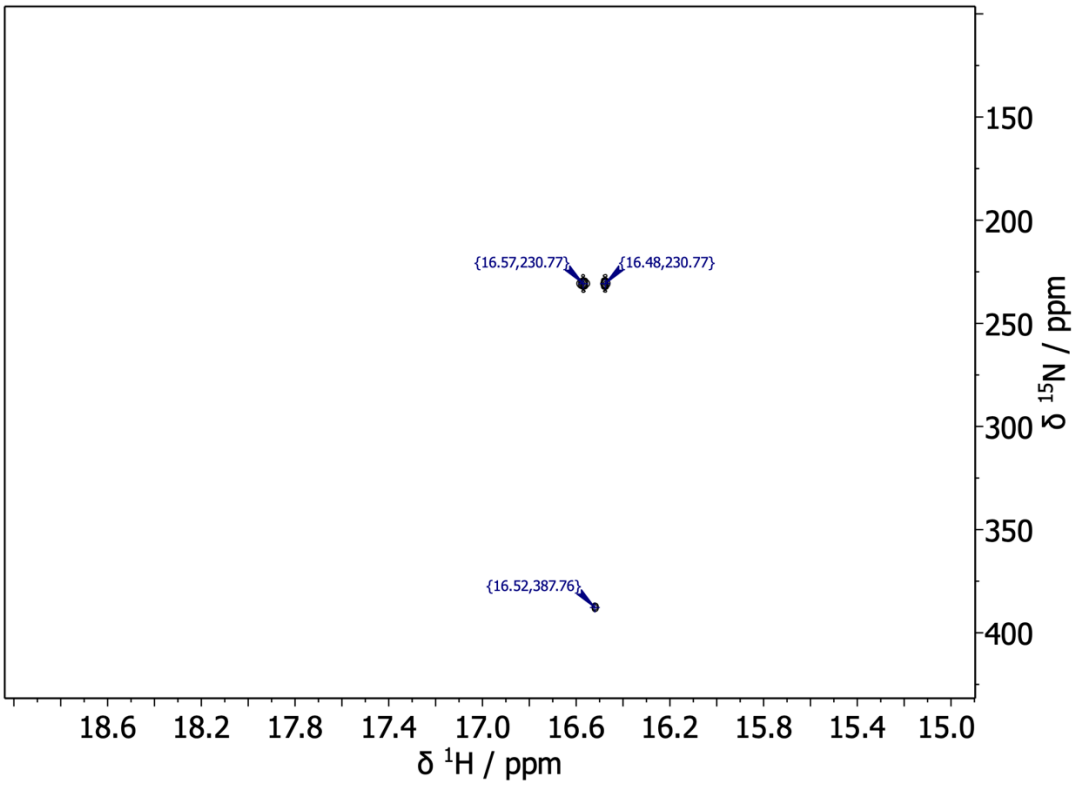

Figure S9. $^{1}H–^{15}N$ HMBC spectrum of ALR at 40 °C, measured in DMF

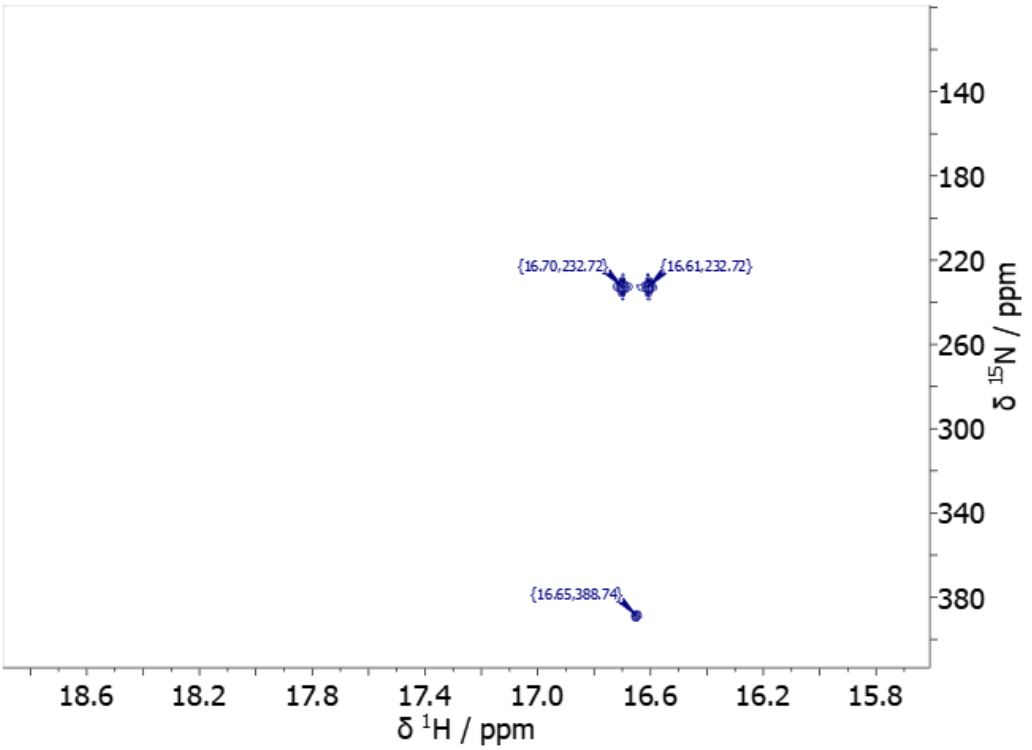

Figure S10. $^{1}H–^{15}N$ HMBC spectrum of ALR at 50 °C, measured in DMF.

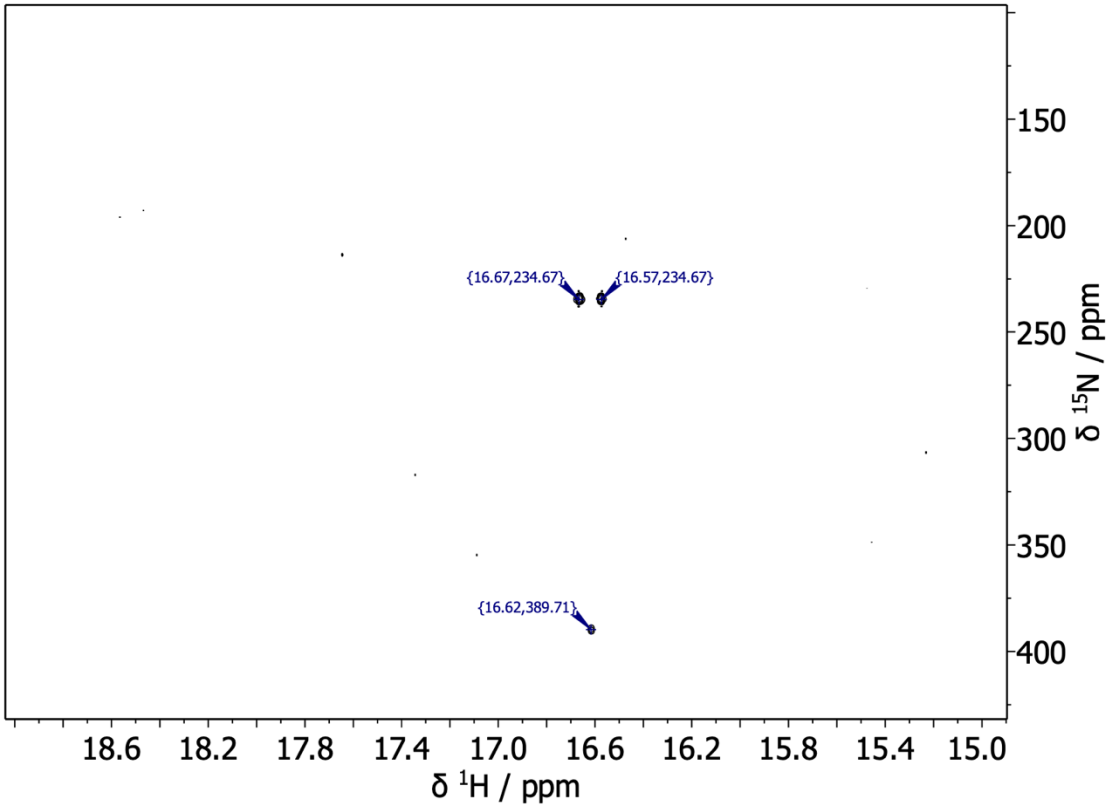

Figure S11. $^{1}H–^{15}N$ HMBC spectrum of ALR at 60 °C, measured in DMF

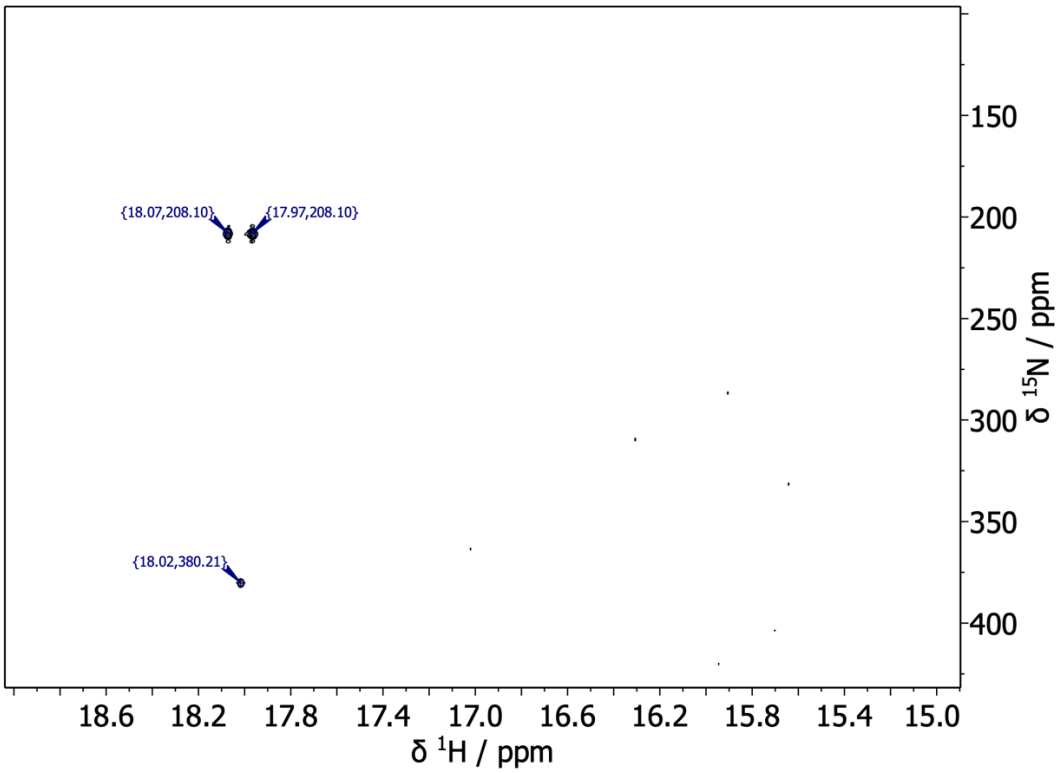

Figure S12. $^{1}H–^{15}N$ HMBC spectrum of AMA at -30.0 °C, measured in DMF

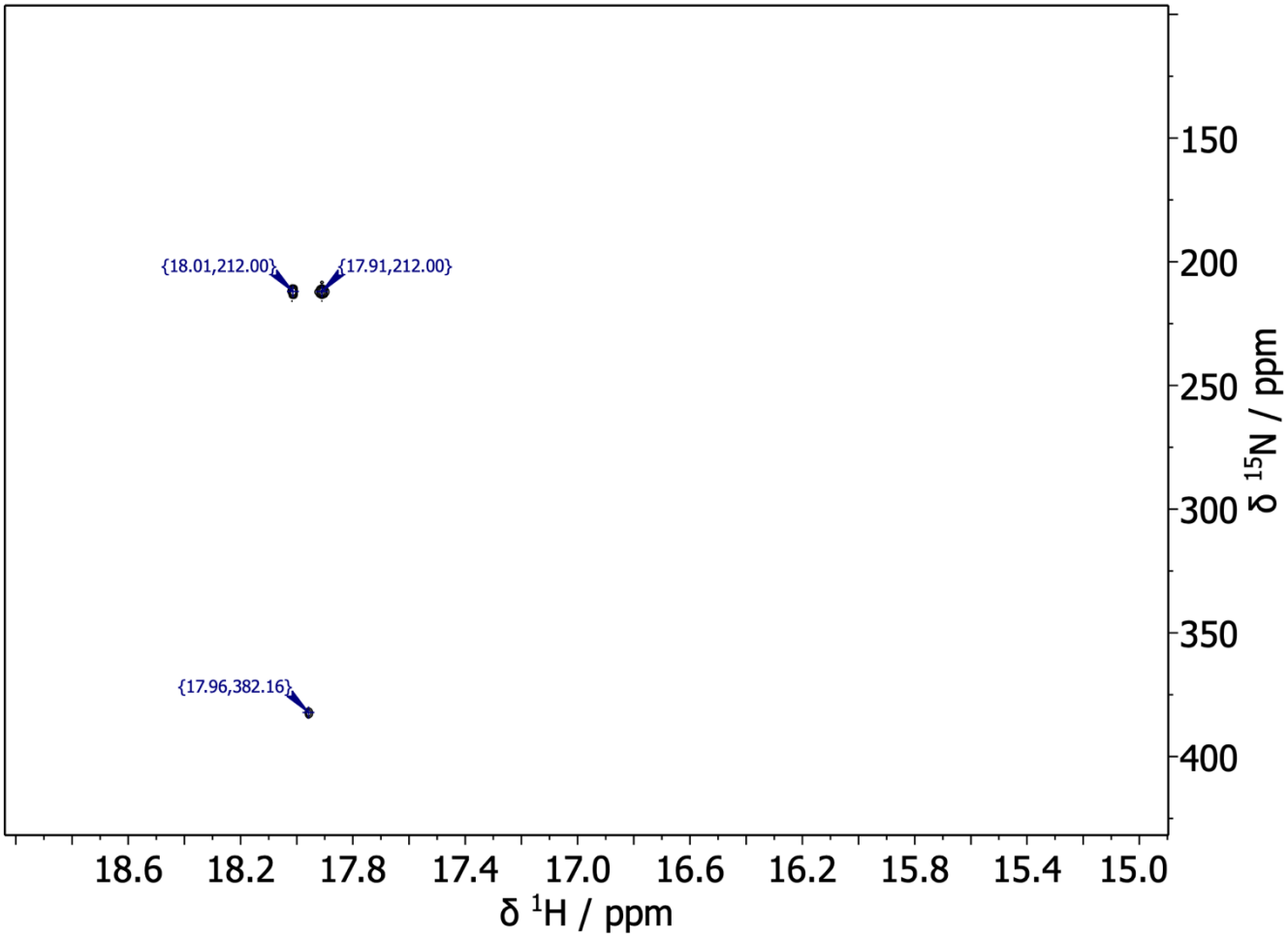

Figure S13. $^{1}H–^{15}N$ HMBC spectrum of AMA at -15.0 °C, measured in DMF

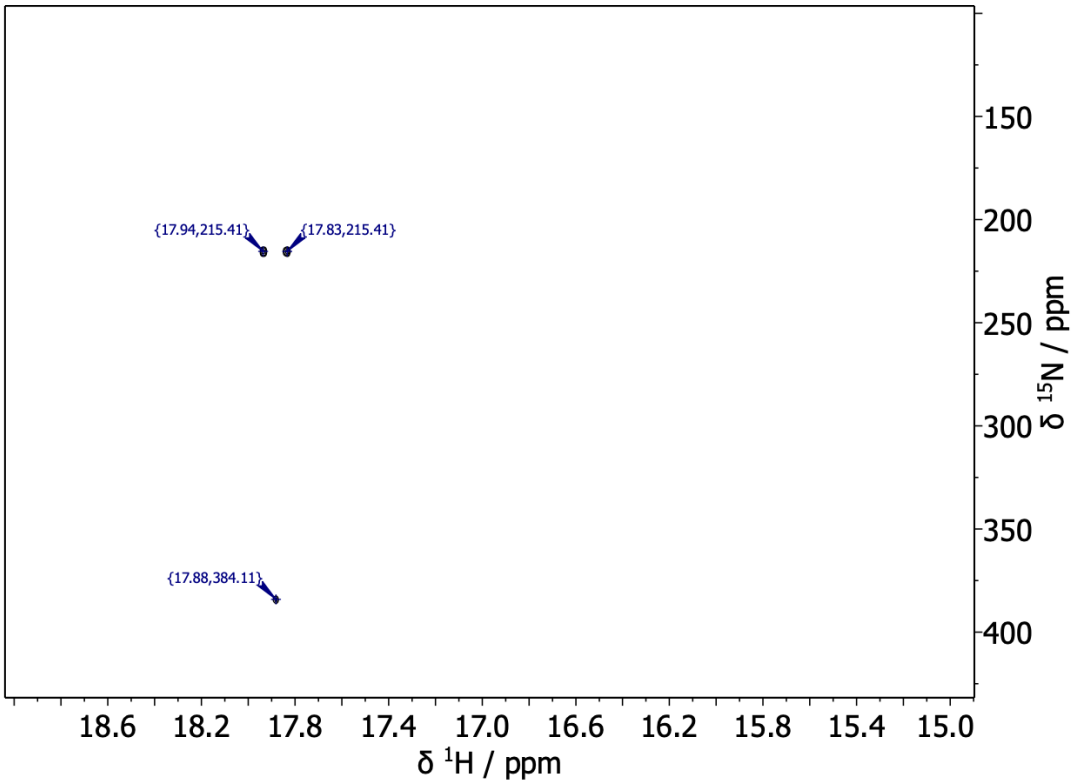

Figure S14. $^{1}H–^{15}N$ HMBC spectrum of AMA at 0.0 °C, measured in DMF

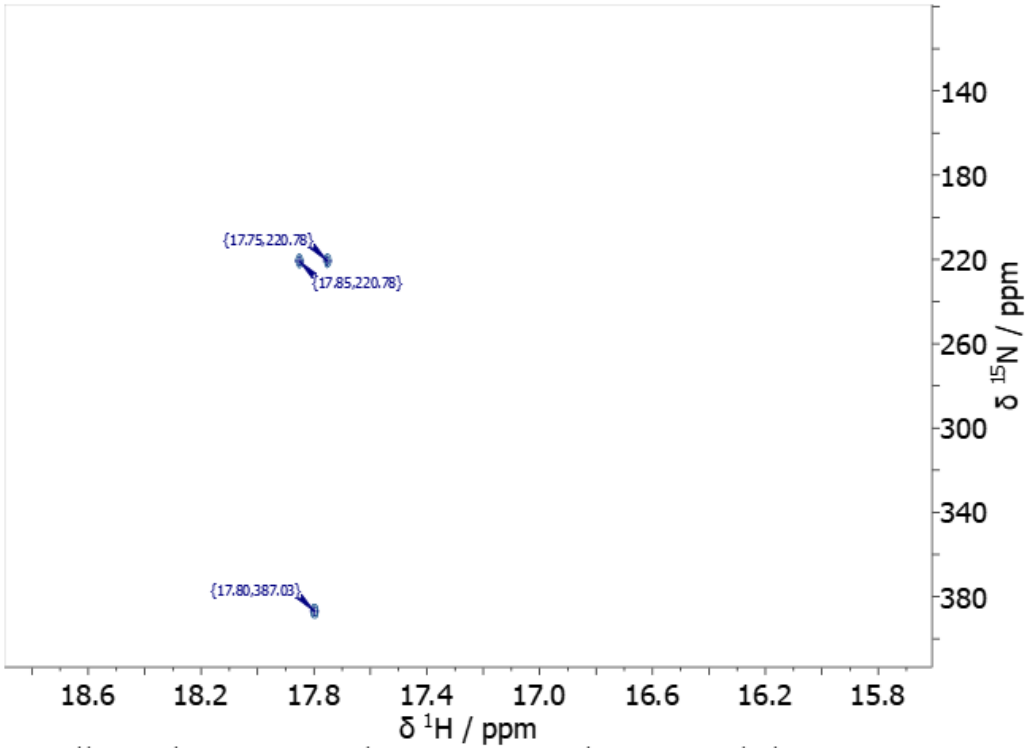

Figure S15. $^{1}H–^{15}N$ HMBC spectrum of AMA at 15.0 °C, measured in DMF

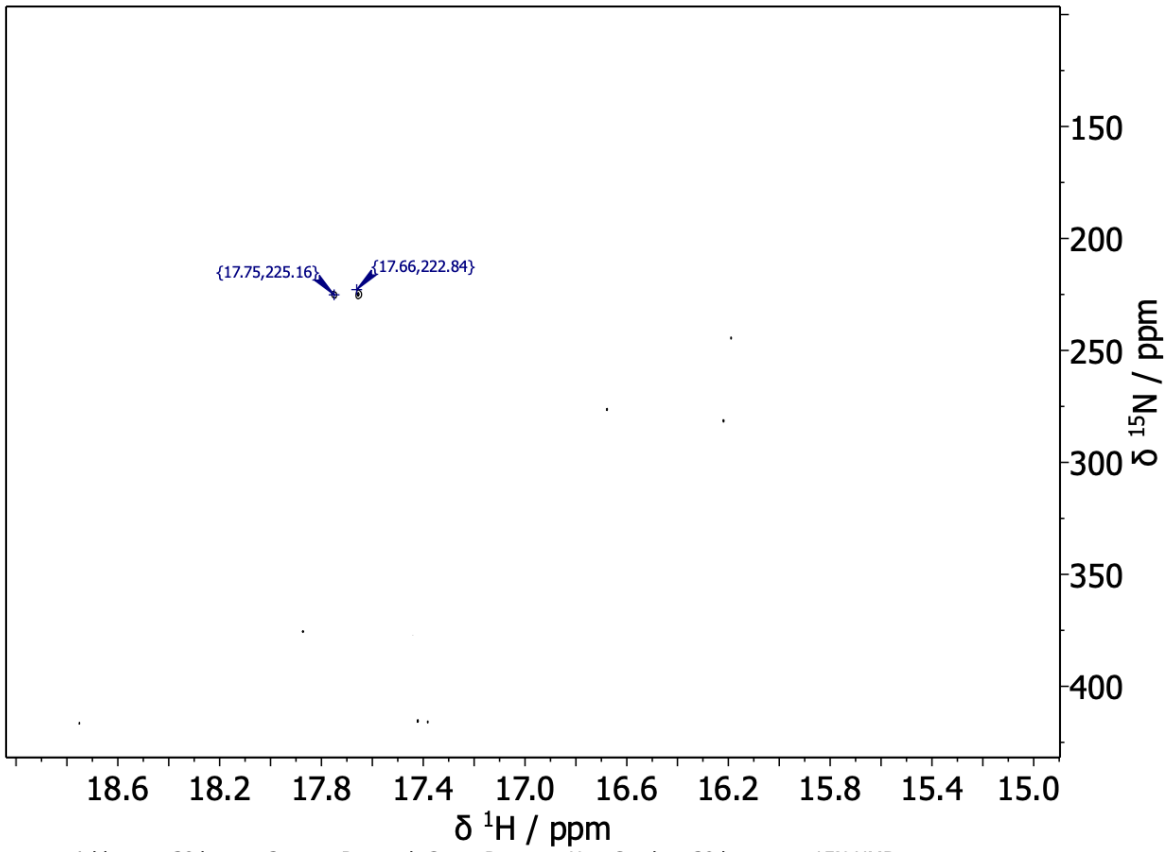

Figure S16. $^{1}H–^{15}N$ HMBC spectrum of AMA at 30.0 °C, measured in DMF

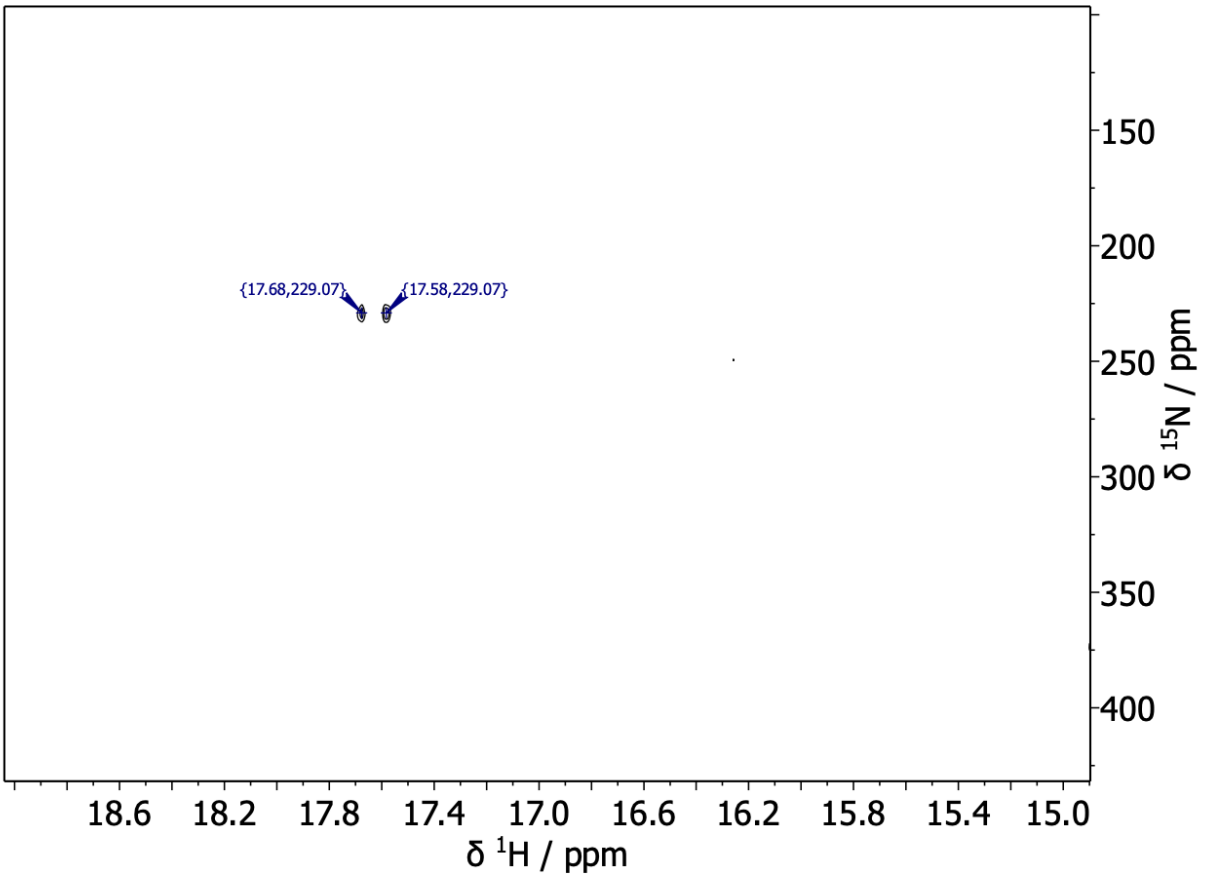

Figure S17. $^{1}H–^{15}N$ HMBC spectrum of AMA at 40.0 °C, measured in DMF

3. ^{13}C CP MAS NMR spectra of ALR, AMA and ALR-, AMA -chitosan films.

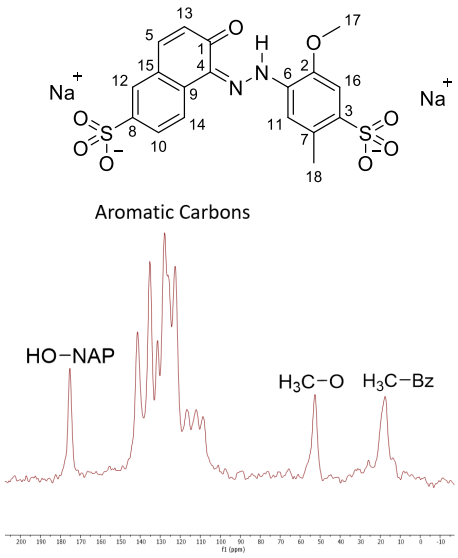

Assignment	PPM
5	141.3
6	134.8
8	131.6
10	127.7
14	122.5
15	116.3
16	112.0
3	108.0

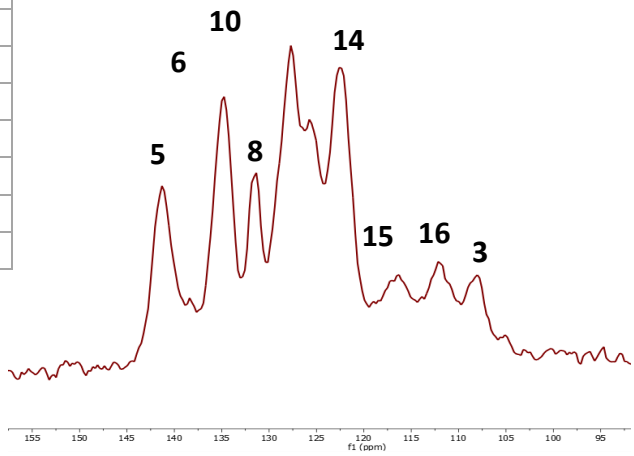

Figure S18. ^{13}C CPMAS NMR spectrum of ALR.

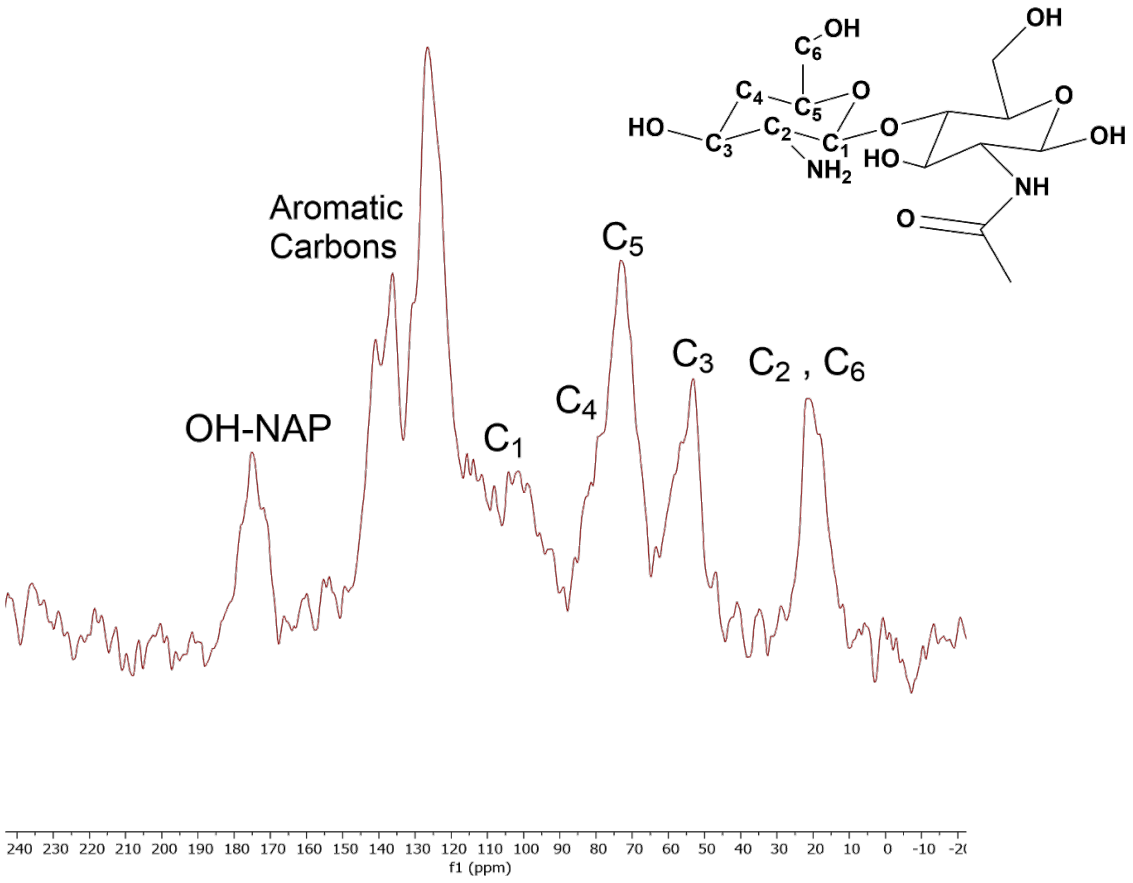

Figure S19 ^{1}H-^{13}C CPMAS NMR spectrum of ALR-Chitosan film.

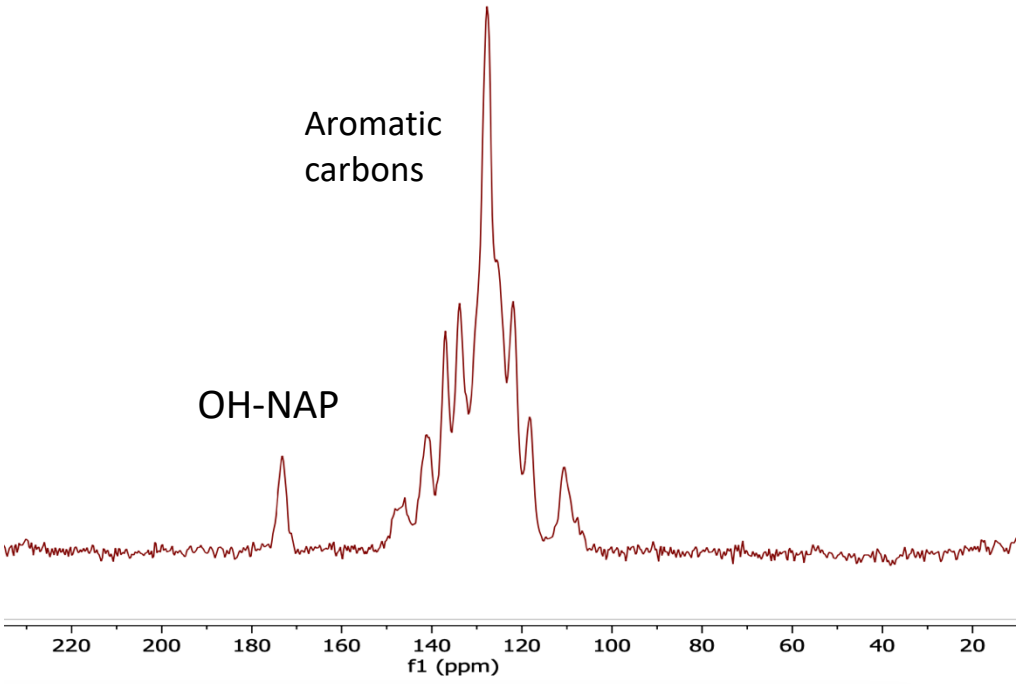

Figure S20 ^{1}H-^{13}C CPMAS NMR spectrum of AMA.

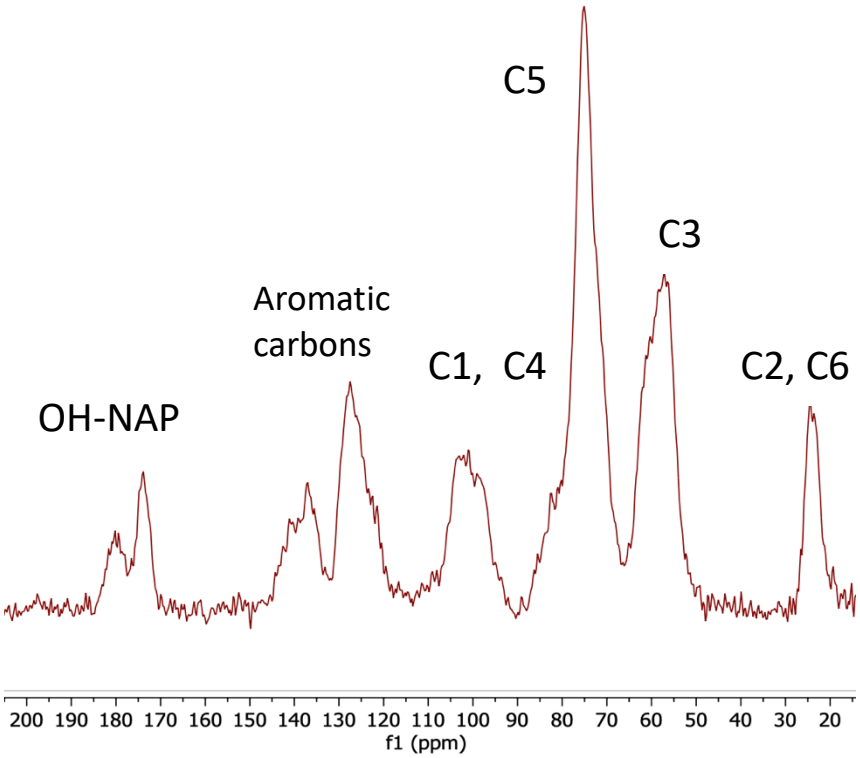

Figure S21 ^{1}H-^{13}C CPMAS NMR spectrum of AMA-Chitosan film

4. Selected abnormal geometry optimizations

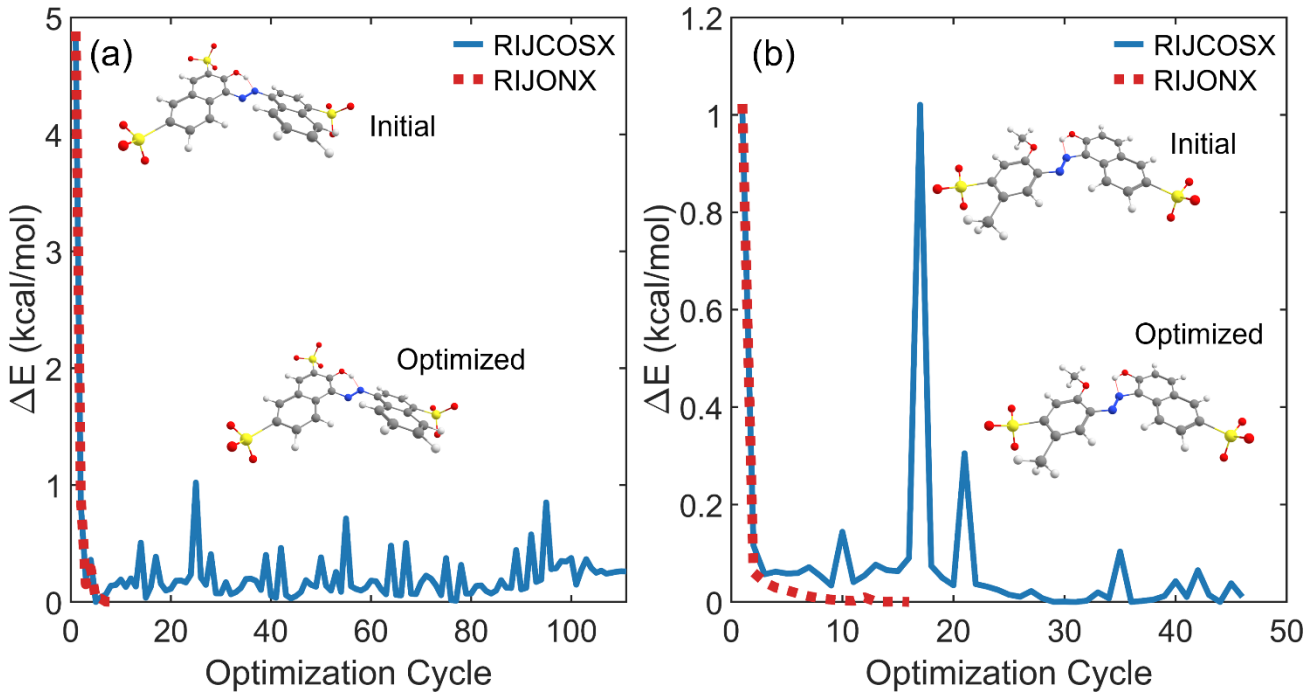

Figure S22. Selected abnormal geometry optimizations of (a) **1d** and (b) **3c** at the M06-2X//def2-TZVP/ma-def2-TZVP level. The plot illustrates significant noise in the optimization when default RI approximation with chain-of-spheres (RIJCOSX) was applied to evaluate exchange and Coulomb integrals, compared to smooth convergence when RI was applied to Coulomb integrals only (RIJONX). The electronic energy is plotted relative to the energy of the optimized geometry, if located; otherwise, the energy is plotted relative to the minimum-energy structure found in the optimization. Initial and final optimized structures are shown overlaid on the plot.

5. Conformations of ALR and AMA

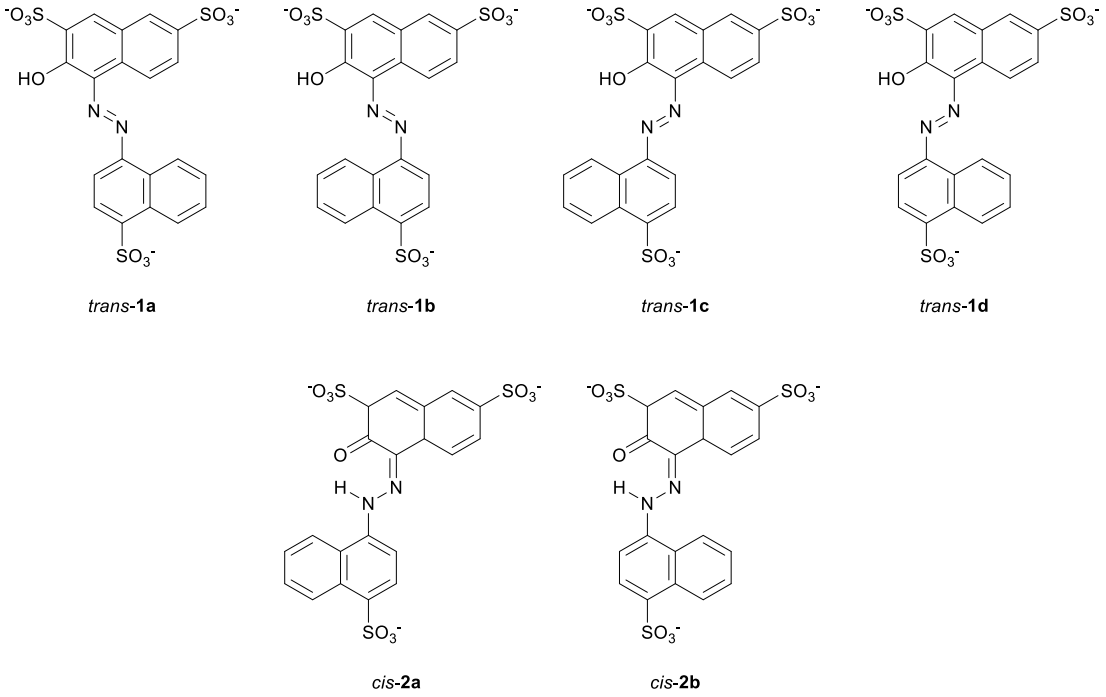

Figure S23. Conformations of the azo (**1**) and hydrazone (**2**) forms of AMA studied in this work.

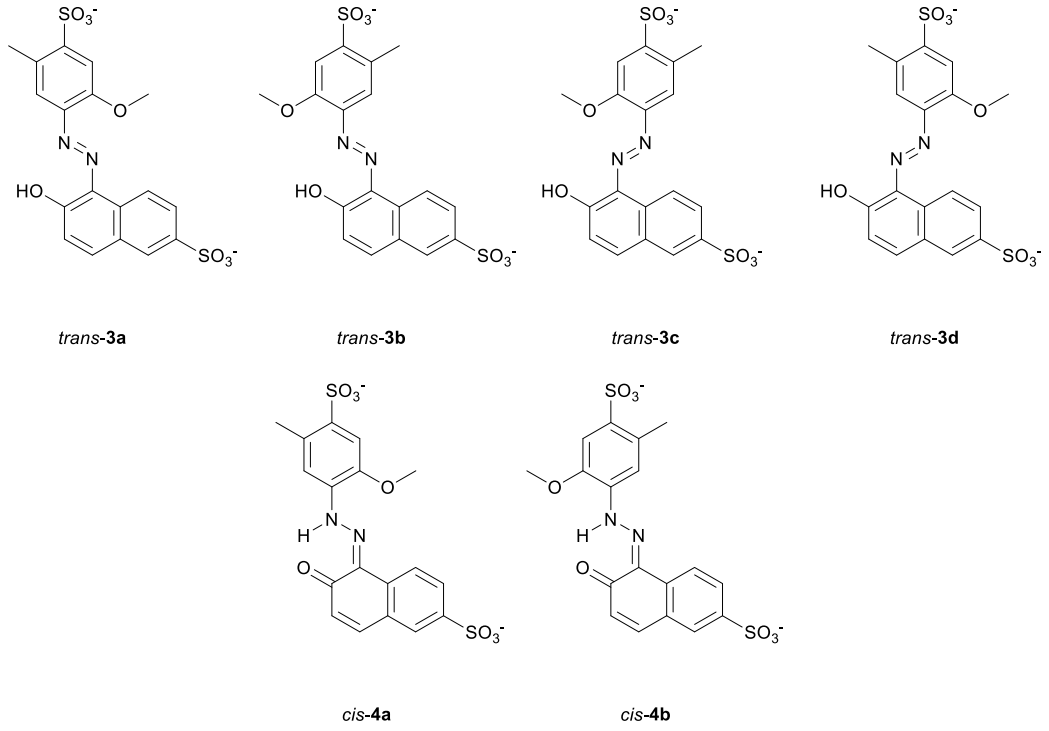

Figure S24. Conformations of the azo (**3**) and hydrazone (**4**) forms of ALR studied in this work.

6. Electronic energies, solvent-free thermodynamic corrections, Gibbs free energies

Table S1. Electronic energies $E_{\text{electronic}}$ of the azo (**1**) and hydrazone (**2**) tautomeric forms of AMA calculated at the M06-2X//def2-TZVP/ma-def2-TZVP level. Solvated electronic energies were calculated by evaluating the solvent-free-optimized geometry in a solvent continuum model (SMD) of DMF.

Conformer	$E_{\text{electronic}}$ (Hartree)			
	Solvent-Free		DMF	
	OH···azo	OH···SO_3^-	OH···azo	OH···SO_3^-
1a	-2825.16992334	-2825.17884219	-2825.57442733	-2825.57834262
1b	-2825.16485893	-2825.17482803	-2825.56998887	-2825.57375573
1c	-2825.17598062	-2825.17996698	-2825.58055438	-2825.57930123
1d	-2825.17138098	-2825.17344463	-2825.57648010	-2825.33502690
2a	-2825.17600165	-	-2825.58134886	-
2b	-2825.17029645	-	-2825.57683878	-

Table S2. Solvent-free thermodynamic corrections $G - E_{\text{electronic}}$ of the azo (**1**) and hydrazone (**2**) tautomeric forms of AMA calculated at the M06-2X//def2-TZVP/ma-def2-TZVP level at temperature 298.15 K and pressure 1 atm.

Conformer	$G - E_{\text{electronic}}$ (Hartree)	
	OH···azo	OH···SO_3^-
1a	0.24690593	0.24636906
1b	0.24662074	0.24589667
1c	0.24650426	0.24601111
1d	0.24668069	0.24605157
2a	0.24609213	-
2b	0.24651173	-

Table S3. Relative Gibbs free energies of the azo (**1**) and hydrazone (**2**) tautomeric forms of AMA calculated at the M06-2X//def2-TZVP/ma-def2-TZVP level, reported with respect to the minimum-energy conformation highlighted in yellow. Solvated relative Gibbs free energies were calculated by adding solvent-free thermodynamic corrections to the electronic energy evaluated in a solvent-continuum model (SMD) of DMF. Boltzmann weights are given in parentheses.

Conformer	ΔG (kJ/mol)			
	Solvent-Free		DMF	
	OH···azo	OH···SO_3^-	OH···azo	OH···SO_3^-
1a	28.7 (0.0000)	3.9 (0.1700)	17.1 (0.0006)	5.5 (0.0703)
1b	41.3 (0.0000)	13.2 (0.0040)	28.1 (0.0000)	16.3 (0.0010)
1c	11.8 (0.0071)	0.00 (0.8181)	0.00 (0.6351)	2.00 (0.2838)
1d	24.3 (0.0000)	17.2 (0.0008)	11.2 (0.0070)	14.1 (0.0022)
2a	0.00 (0.9985)	-	0.00 (0.9946)	-
2b	16.1 (0.0015)	-	12.9 (0.0054)	-

Table S4. Electronic energies $E_{\text{electronic}}$ of the azo (**3**) and hydrazone (**4**) tautomeric forms of ALR calculated at the M06-2X//def2-TZVP/ma-def2-TZVP level. Solvated electronic energies were calculated by evaluating the solvent-free-optimized geometry in a solvent continuum model (SMD) of DMF.

Conformer	$E_{\text{electronic}}$ (Hartree)	
	Solvent-Free	DMF
3a	-2202.12247922	-2202.33811236
3b	-2202.12812080	-2202.34393799
3c	-2202.11676370	-2202.33292080
3d	-2202.11744964	-2202.33502690
4a	-2202.12048340	-2202.33719510
4b	-2202.12814586	-2202.34488463

Table S5. Solvent-free thermodynamic corrections $G - E_{\text{electronic}}$ of the azo (**3**) and hydrazone (**4**) tautomeric forms of ALR calculated at the M06-2X//def2-TZVP/ma-def2-TZVP level at temperature 298.15 K and pressure 1 atm.

Conformer	$G - E_{\text{electronic}}$ (Hartree)
3a	0.25823637
3b	0.25813078
3c	0.25793885
3d†	0.25976883
4a†	0.25942622
4b	0.25846243

†Vibrational analysis returned a single imaginary mode corresponding to a shallow-well rotation of the methyl and sulphonate groups on the phenyl ring. Attempts to re-optimize changed the energy by less than 2 kJ/mol and, given the minimal contribution of these structures (Boltzmann weights ~ 0.0000), no further attempts were made to remove these imaginary modes.

Table S6. Relative Gibbs free energies of the azo (**3**) and hydrazone (**4**) tautomeric forms of ALR calculated at the M06-2X//def2-TZVP/ma-def2-TZVP level, reported with respect to the minimum-energy conformation highlighted in yellow. Solvated relative Gibbs free energies were calculated by adding solvent-free thermodynamic corrections to the electronic energy evaluated in a solvent-continuum model (SMD) of DMF. Boltzmann weights are given in parentheses.

Conformer	ΔG (kJ/mol)	
	Solvent-Free	DMF
3a	15.1 (0.0023)	15.6 (0.0019)
3b	0.00 (0.9977)	0.00 (0.9981)
3c	29.3 (0.0000)	28.4 (0.0000)
3d†	32.3 (0.0000)	27.7 (0.0000)
4a†	22.7 (0.0001)	22.7 (0.0001)
4b	0.00 (0.9999)	0.00 (0.9999)

†Vibrational analysis returned a single imaginary mode corresponding to a shallow-well rotation of the methyl and sulphonate groups on the phenyl ring. Attempts to re-optimize changed the energy by less than 2 kJ/mol and, given the minimal contribution of these structures (Boltzmann weights ~ 0.0000), no further attempts were made to remove these imaginary modes.

7. Natural bond orders

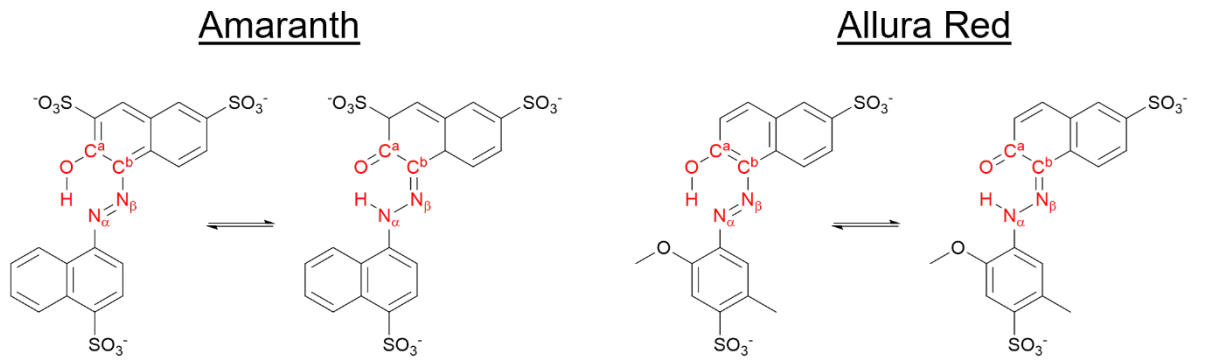

	Solvent-Free		DMF	
	Azo	Hyd	Azo	Hyd
C^a-O	0.82	1.27	0.83	1.26
C^b-N_β	0.92	1.62	0.97	1.59
N_α-N_β	1.87	1.09	1.75	1.11
O-H	0.41	-	0.40	-
N_α-H	-	0.49	-	0.49

	Solvent-Free		DMF	
	Azo	Hyd	Azo	Hyd
C^a-O	0.81	1.24	0.82	1.24
C^b-N_β	0.95	1.51	0.95	1.52
N_α-N_β	1.78	1.16	1.78	1.15
O-H	0.40	-	0.40	-
N_α-H	-	0.48	-	0.48

Figure S25. Natural bond orders from natural localized molecular orbitals for the azo and hydrazone forms of AMA and ALR calculated at the M06-2X//def2-TZVP/ma-def2-TZVP level in solvent-free conditions and a solvent continuum model (SMD) of DMF.